T.3: Studies on generation and manipulation of laser cooled atoms

S. P. Ram
Laser Physics Applications Section
Email: spram@rrcat.gov.in

Abstract

This article describes the development and operation of a double magneto-optical trap (MOT) setup for generation of ultracold ^{87}Rb atoms. The transfer of atoms from a vapor chamber MOT (VC-MOT) to an ultra-high vacuum MOT (UHV-MOT) has been extensively studied. A push beam has been used for transfer of atoms from the VC-MOT to the UHV-MOT in different geometries and configurations to maximize the number of atoms in the UHV-MOT. The results of a resonant push beam in presence of a counter-propagating weakly focused hollow beam have been presented here. The investigations during this work also revealed that use of a red-detuned (and higher power) continuous wave push beam of an optimized spot-size results in much higher number of atoms in the UHV-MOT. Further, the transfer of laser cooled atom cloud from UHV-MOT to a magnetic trap has also been studied during the course of the work. The optimization of magnetic field gradient during switching on of the magnetic trap, for maximizing phase space density and its dependence on the temperature and r.m.s. size of the laser cooled atom cloud in the UHV-MOT and molasses has been investigated. To generate the ultracold atomic samples of ^{87}Rb, the evaporative cooling of laser cooled ^{87}Rb atoms in a quadrupole-Ioffe configuration (QUIC) magnetic trap has been performed. After evaporative cooling, a bimodal distribution in the optical density profile of the evaporatively cooled atom cloud was observed which indicated the occurrence of Bose-Einstein condensation (BEC) in the atom cloud.

1. Introduction

Over the last few decades there has been a phenomenal progress in the field of ultra-cold atoms [1, 2]. The field has seen amazingly new developments, which include ultra-precision spectroscopy [3-5], quantum optics [6, 7], ultra-cold collision physics [8], cold molecules [9], matter wave optics [10], ultra-cold plasmas [11] and most importantly Bose-Einstein condensation (BEC) [12-14]. Experimental realization of BEC [15-17] is, perhaps, the landmark accomplishment of ultra-cold atom research and that has led to an explosive growth of research in quantum degenerate gases including metastable and fermionic atoms, superfluidity, quantized vortices, Josephson junction, quantum phase transitions etc. [13]. It has also provided an opportunity to study the wave particle duality of matter and has formed the basis of research in non-linear and quantum atom optics. The applications of laser-cooled atoms are equally fascinating and include, for example, precision atomic clocks [1], ultra-precise gravity gradiometer [5], atom lithography [14] and quantum information processing [6]. Underlying this explosive growth are the innovative techniques of generation and manipulation of ultra-cold atoms.

1.1 Fundamentals of laser atom cooling and trapping

In the context of laser cooling the temperature describes the spread in velocities in an atomic distribution (Maxwell-Boltzmann distribution). From the kinetic theory of gases in 1D, we can relate the thermal energy of the atoms to the v_{rms} (the velocity spread in a Maxwell-Boltzmann distribution) as follows,

$$\frac{1}{2}k_B T = \frac{1}{2}m v_{rms}^2$$

where k_B is Boltzmann's constant, T is the temperature and m is the atomic mass. Therefore reducing the v_{rms}, ultimately leads to reduction in the temperature. The average velocity of atoms reduces to few mm/s from few hundred m/s by laser cooling technique.

Light can be used as a tool to manipulate and control the external degrees of freedom of an atom, i.e. position and momentum of the atom and the internal states of the atoms. The cycle of unidirectional absorption of photons from a laser beam and spontaneous emission of photons in random direction lead to transfer of momentum of photons to the atom. This results in a force called “scattering force” or “radiation pressure force”. This scattering force can give a maximum deceleration of $\sim 10^5 g$ (g is the acceleration due to gravity), which clearly shows the potential of the resonant laser light acting on atoms. Another kind of force arises from laser induced dipole moment of atom and its interaction with the laser field. Its magnitude is dependent on the spatial derivative of the intensity profile of the laser beam and the detuning of the laser beam from the atomic resonance. Because of this, this force is called “gradient force” or “dipole force”. These two forces can be used to manipulate the atomic motion. The scattering force which is dissipative in nature, can be made velocity dependent and hence becomes useful for cooling of atoms. The dipole force is useful for trapping and guiding of cold atoms.

The scattering force of laser beam on atom can be utilized to

reduce the speed of the atoms. The Doppler cooling is one such mechanism which exploits the Doppler effect to generate the cooling effect of laser beam on an atom. An atom under motion with a particular velocity can be in the resonance with the oppositely propagating laser beam when the Doppler shifted frequency of laser beam experienced by the atom equals the atomic transition frequency. As a result, the laser beam can exert a net force on the atom which can reduce its velocity. Such scattering force is detuning dependent and is velocity dependent as well. Exploiting this, T.W. Hänsch and A.L. Schawlow have proposed using three pairs of counter-propagating red-detuned beams to cool atoms and Chu et al has experimentally realized this Doppler cooling. This geometry has been popularly known as "optical molasses".

Though the cooling of atoms in optical molasses helps in reducing the kinetic energy, it lacks to provide any spatial confinement. Due to lack of trapping or confinement, the atom may diffuse out of the overlapping region with time. Also, the effectiveness of cooling in molasses depends upon the detuning which becomes larger with cooling of atoms. After cooling, an atom may reach to a velocity range where the Doppler shift no longer brings the atom to the resonance and hence the cooling ceases.

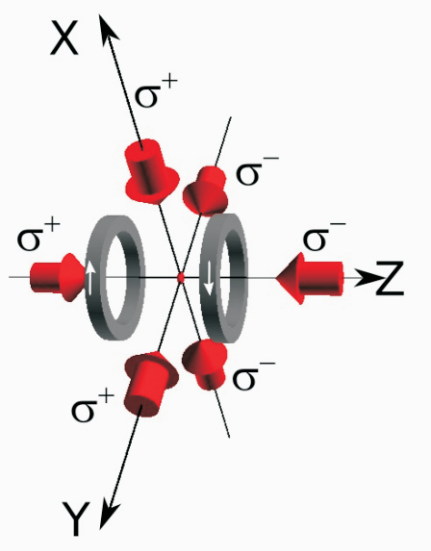

Fig. T.3.1: Configuration of magneto-optical trap (MOT). Three pairs of laser beams of equal intensity and frequency in conjunction with an inhomogeneous field generated by a pair of coils in quadrupole configuration is used for formation of MOT.

To circumvent these problems an inhomogeneous magnetic field (generated by a quadrupole coils) is superposed which introduces a position dependent scattering force. This configuration is known as magneto-optical trap (MOT) as shown in Figure T.3.1 and due to the simplicity and robustness of MOT, it has become a widely used source of cold atoms. In the MOT, three pairs ($\sigma^+ - \sigma^-$) of laser beams are used. A spherical quadrupole field is superimposed in such a way that its center matches with the intersection point of the beams. For an appropriate combination of magnetic field and laser beam polarization, an atom moving away from the center will experience a force directing it towards the center of the trap. MOT provides a trap capable of accumulating large number of atoms, but the temperature and density that can be achieved is limited due to a number of reasons [1,12-14]. To increase the density a very convenient stage is compressed MOT (CMOT), performed by increasing the detuning of the cooling laser and increasing the field gradient used for MOT. As a result, the radiation pressure reduces which increases the density of atoms in MOT. Further, to lower the temperature of atoms in MOT, the magnetic field is turned off to leave the atoms in optical molasses, where sub-Doppler cooling mechanisms can take place. To further lower the temperature achieved by MOT, CMOT and optical molasses stages, another cooling stage "evaporative cooling" is necessary. Evaporative cooling is a method to reach the temperature below the temperature regimes achievable by laser cooling technique. The idea of evaporative cooling was introduced by Hess for hydrogen [12-14]. But this technique proved to be very useful in alkali atoms to reach the quantum degeneracy [15]. In magnetic traps it is implemented by using radio frequency (RF) radiations [18]. The principle is as follows: the atoms with higher energy are selectively removed from the trap by applying the RF radiation. The RF radiation makes the atoms flip the spin and pumped to an untrappable state and hence, leave the trap. As a result, rest of the atoms in the trap thermalize to a lower temperature by elastic collision. The evaporative cooling can be performed in a trap where the atoms can be stored for a longer time. The quadrupole trap generates a potential of V shape with a minimum (zero) at the center. The main problem with the quadrupole trap is the zero field at the center where atoms may make a spin flip (Majorana flip) and go to untrappable state and hence may be lost from the trap [12-14]. For this reason the quadrupole trap is not suitable for evaporative cooling which requires a longer life-time of the trap. For evaporative cooling purpose, various techniques are employed to eliminate the Majorana spin flip losses. These include "plug the hole", "time orbiting potential (TOP) trap", "the Ioffe-Pritchard trap", "the cloverleaf trap", "the base ball trap", "quadrupole-Ioffe configuration (QUIC)

trap" etc. [12-14, 19-21]. When the temperature is lowered by evaporative cooling, below a certain temperature and for a particular density of atoms, macroscopic accumulation of atoms in lowest energy state takes place. This special phenomena occurs only for Bosons (particles having integral spin) and is known as Bose-Einstein condensation (BEC). The temperature below which BEC occurs is known as critical temperature.

2. Experimental apparatus

The experimental realization of laser cooling and evaporative cooling is a challenging task as they require different pressure regimes. A setup, comprising of two chambers having different vacuum levels acting as vapor chamber (made of stainless steel) and ultra-high vacuum chamber (glass cell), is developed for achieving laser cooling and evaporative cooling of ^{87}Rb atoms. The setup is known as double-MOT setup [22] as shown in Figure T.3.2. An image of the setup is shown in Figure T.3.3. A suitably designed differential pumping tube is used to maintain the pressure level in the chambers. The double-MOT setup is very convenient to implement the two stage cooling of atoms. The laser cooling stage results typically the temperature of cold atoms in the range 50 - 500 μK, whereas the evaporative cooling can result the temperature in the range of sub-micro-Kelvin to few micro-Kelvin. Here, laser cooling of ^{87}Rb atoms in the magneto-optical traps (MOTs) provides the first stage of cooling and evaporative cooling of these laser cooled samples in a magnetic trap leads to the second stage of cooling. For realization of the two stage cooling process, the apparatus consists of several frequency stabilized laser systems, magnetic traps for cold atoms, RF evaporative cooling systems, detection and characterization equipments, and a PC-based controller system to implement various cooling stages in a desired sequence.

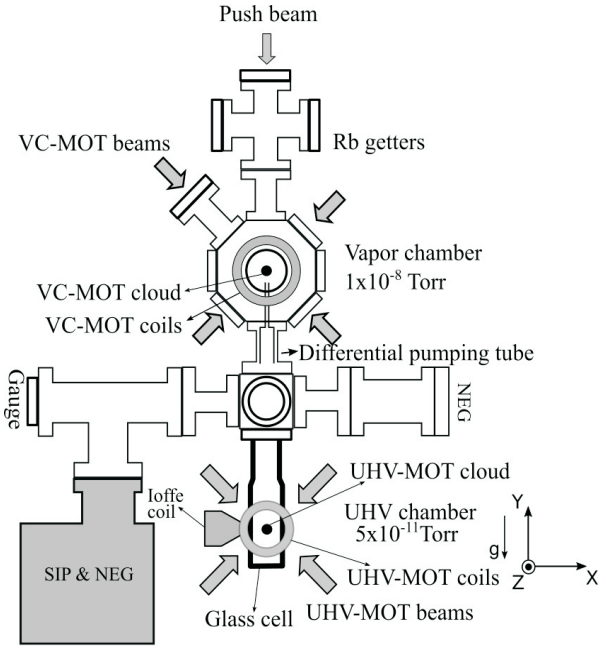

Fig. T.3.2: Schematic of the experimental double MOT setup.

In the double-MOT setup, one of the chamber is at a pressure ~1 × 10^{-8} Torr (with Rb-vapor) where the first MOT of ^{87}Rb atoms is formed by collecting the atoms from the background Rb-vapor in this chamber. This MOT is known as vapor chamber MOT (VC-MOT). The second MOT is formed in a different chamber kept at an ultra-high vacuum (UHV) (~6 × 10^{-11} Torr) environment. The second MOT is known as UHVMOT for which the Rb atoms from the VC-MOT act as a source. The atoms collected in the UHV-MOT are used for magnetic trapping and evaporative cooling to generate atomic samples having further lower temperature. The UHV environment in the chamber is suitable for the long life-time

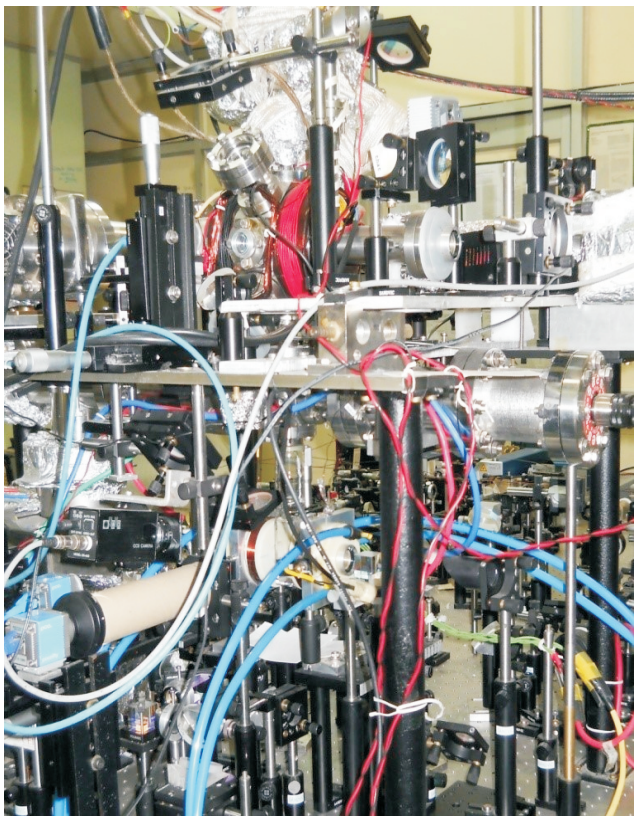

Fig. T.3.3: A photograph showing the double MOT setup.

of atoms in the magnetic trap which is necessary for the evaporative cooling process due to its slow nature.

3. Atom transfer with resonant push beam

The collection of a large number of atoms in UHV-MOT in the double-MOT setup is quite important. Various methods are employed for transfer of atoms from a VC-MOT to UHV-MOT [23,24]. Several groups have used a push beam to eject the flux of atoms from the VC-MOT for loading of the UHV-MOT. The use of push beam for transfer of atoms is a simple and convenient technique. We have chosen to investigate the transfer of atoms from VC-MOT to UHV-MOT using a resonant push beam, which is resonant to $(5S_{1/2}\,F=2)\rightarrow(5P_{3/2}\,F'=3)$ transition of ^{87}Rb. We have used the push beam in different schemes. First, we have studied the effect of using an auxiliary hollow beam in conjunction to a low power resonant push beam.

3.1 Use of a hollow laser beam in conjunction with the resonant push beam

A hollow beam is used to enhance the atom transfer between VC-MOT and UHV-MOT. In this scheme, a weakly focused hollow laser beam was aligned to propagate opposite to the direction of the push beam. The hollow beam was aligned in such a way that the atomic flux ejected from VC-MOT, both the MOTs were in the dark region of the hollow beam.

The push beam was a continuous wave Gaussian laser beam resonant with $(5S_{1/2}\,F=2)\rightarrow(5P_{3/2}\,F'=3)$ transition of ^{87}Rb. It was focused to $1/e^2$ size ~ 100 µm at the VC-MOT position, which corresponded to a push beam intensity at VC-MOT of ~10^3 mW/cm^2 and at UHV-MOT ~ 13 mW/cm^2 for a power of ~ 150 µW. Atoms ejected from the VC-MOT by the push beam were captured in the UHV-MOT. A weakly focused hollow laser beam propagating vertically upwards was aligned such that both the MOTs were in its dark central region. The hollow beam was generated using a homemade metal axicon mirror. The peak to peak intensity diameter and ring-width (FWHM) of the hollow beam were, ~ 14.3 mm and ~ 1.4 mm at the UHV-MOT and ~ 3.2 mm and ~ 1.24 mm respectively, at the VC-MOT. This corresponds to peak intensities ~ 50 mW/cm^2 and ~230 mW/cm^2 at UHV-MOT and VC-MOT plane respectively, for a beam power of 30 mW.

The variation in the number of atoms in the UHV-MOT in presence of hollow beam (N_p) with the frequency of the hollow beam was measured. We have also measured the number of atoms in the UHV-MOT in absence of the counter-propagating hollow beam (N_a). The results are shown in Figure T.3.4. The experimental results have shown a significant enhancement in the number of atoms in the UHV-MOT in presence of the hollow beam (N_p) when it was tuned appropriately. The observed enhancement in number of atoms in the UHV-MOT has been attributed to the cooling and transverse guiding of flux of atoms reaching the UHV-MOT due to interaction of atoms in the flux with the hollow beam.

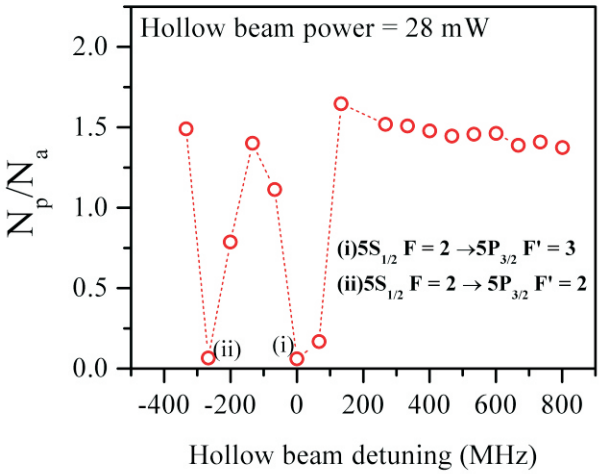

Fig. T.3.4: Measured variation in the ratio of number of atoms in UHV-MOT in presence (N_p) and absence (N_a) of hollow beam with the detuning of the hollow beam frequency.

The investigations have suggested that the increase was due to decrease in average speed of flux of atoms from VC-MOT as well as increase in number of atoms reaching the capture volume of the UHV-MOT due to the presence of the hollow beam. The additional effect of the hollow beam on the atom flux from the VC-MOT could be the reduction in divergence of the flux because of transverse cooling and guiding effects of the beam.

4. Atom transfer with red-detuned push beam

The detuning of a laser beam with respect to the atomic resonance frequency governs, whether an atom will be pushed towards the higher intensity (for red-detuned) or towards the lower intensity (for blue-detuned). This behaviour arises due to the dipole force [1,12-14] experienced by the atoms. This dipole force is also helpful in guiding of atoms from one position to other. The guiding improves the efficiency in decreasing the transverse temperature during transfer of atoms. Therefore it seems beneficial, if the guiding of atoms can be coupled with the atom transfer between two MOTs using a push beam. Dimova et al. [26] has proposed and demonstrated a technique which used the pushing and

guiding of atoms during the transfer of atoms from one MOT to another in a double-MOT setup. We have proposed and demonstrated that a single beam of sufficiently high power (few tens of mW) and with detuning in the order of few GHz to the red of atomic resonance transition can be used not only for generating a leak in the VC-MOT for extraction of atoms for transfer to UHV-MOT but also for guiding the atoms to the trapping volume of UHV-MOT to load the UHV-MOT [25]. Since guiding is intensity dependent process we have investigated the benefits of using a red-detuned push beam in retro-reflection geometry which enhances the guiding potential of the beam [25]. Further extension in the study of atom transfer with red-detuned push beam was made towards the investigation of the effect of variation in the push beam spot-size at VC-MOT on number of atoms accumulated in UHV-MOT [27].

4.1 Use of a red-detuned push beam in retro-reflecting geometry

Since guiding dipole potential is intensity dependent, one can enhance the above guiding assisted transfer by using the push beam of a given power in retro-reflection geometry, where retro-reflected push beam potential was added (with appropriate sign) to the potential of the forward push beam to give the resultant higher guiding potential. At the same time, the destructive scattering force of forward push beam at UHV-MOT was balanced by that of the retro-reflected push beam. The push beam can confine more atoms in the flux from the VC-MOT to the UHV-MOT in the presence of retro-reflected beam. On the other hand, the resultant scattering force in presence of retro-reflected push beam is reduced because of opposite directions of forces due to forward and retro-reflected components of push beam. This reduced scattering force and increased dipole potential due to push beam are likely the cause of observed higher number in UHV-MOT for the push beam in retro-reflection geometry than the number observed without retro-reflection of the push beam. The higher intensity of the retro-reflected beam provides a higher resultant dipole potential and lower resultant scattering force of the push beam at UHV-MOT atom cloud, both favorable for higher number of atoms in the UHV-MOT. The measured variations in the number of atoms in the UHV-MOT in presence and absence of the retro-reflecting push beam with push beam detuning is shown in Figure T. 3.5. As compared to without retro-reflected push beam, for push beam power of ~ 20 mW, ~ 30 % increase in number in UHV-MOT is observed, when the retro-reflecting mirror is kept a 55 mm distance from the UHV-MOT position.

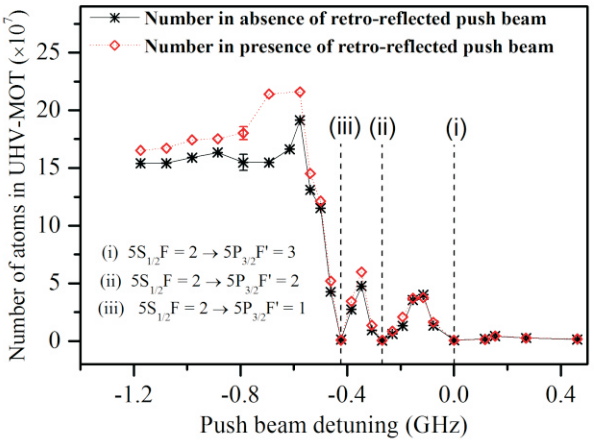

Fig. T.3.5: Measured variation in number of atoms in the UHV-MOT with the frequency detuning of the push beam.

4.2 Dependence of red-detuned push beam spot-size on atom transfer

In this work, the effect of push beam spot-size and power on the number of atoms accumulated in the UHV-MOT has been studied during the atom transfer from the VC-MOT to UHV-MOT. It has been observed that, at a given push beam power, the number of atoms collected in the UHV-MOT varies with the push beam spot-size at the VC-MOT and attains a maximum value at an optimum push beam spot-size. At a given push beam power, the number of atoms accumulated in the UHV-MOT and the optimum push beam spot-size are dependent on the capture speed of the UHV-MOT. The studies have been extended further to investigate the effect of spot-size of red-detuned push beam at VC-MOT on the number of atoms transferred to UHV-MOT. It has been found that at a given power in push beam, number of atoms in UHV-MOT first increases with increasing spot-size and then decreases with it, after attaining a maximum value. The number finally achieved in UHV-MOT is sensitive to spot-size and power of push beam at VC-MOT and capture speed of UHV-MOT. The measured variation in the number of atoms in the UHV-MOT with the spot-size of the push beam at VC-MOT position for various powers of push beam is shown in Figure T. 3. 6.

The velocity of the atoms ejected from VC-MOT, is dependent on intensity (spot-size for a given power). This velocity should be less than the capture velocity of the UHV-MOT. At a lower power and smaller spot-size, the ejected atoms from the VC-MOT is less and hence a lesser number in the UHV-MOT. However, a higher power and larger spot-size result in a poor loading of the source VC-MOT and hence a poor loading of UHV-MOT. Therefore, there exists an

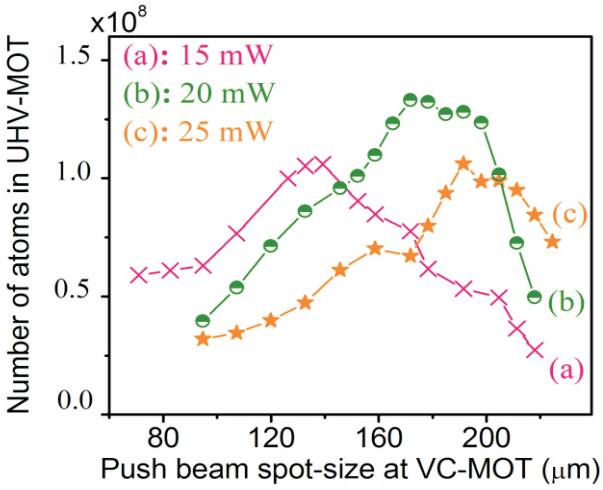

Fig. T.3.6: Measured variation in number of atoms in the UHV-MOT with the spot-size of the push beam at the VC-MOT position for various powers in the push beam.

optimum power and spot-size where the number of the atoms in the UHV-MOT is optimum.

5. Magnetic trapping of laser cooled ^{87}Rb atoms and evaporative cooling in the magnetic trap

The first demonstration of magnetic trapping of neutral atoms proved to be an instrumental idea in achieving the Bose-Einstein condensation (BEC) of alkali atoms in a magnetic trap after evaporative cooling [13, 15–18]. For trapping of cold neutral atoms several designs of magnetic traps have been proposed and demonstrated [13]. The trap depth of the potential generated by the magnetic field determines the kinetic energy of the atoms trappable in the trap. As the potential scales as $\mu_B B$ (where μ_B is the Bohr magneton and B is the magnetic field of the trap), the trap depth has the order of B times the ratio of μ_B/k_B (~ 67 μK/G). It is important to note here that the wall of the UHV-MOT glass cell in our setup acts as a boundary of the trap, where the field is normally of the order of 200 G (assuming the field gradient in quadrupole trap ~ 155 G/cm in our setup), which results in a trap depth of ~ 13 mK. Therefore, pre-cooling of the atoms is a basic requirement for magnetic trapping. We have initially cooled the atoms in an UHV-MOT and then transferred these UHV-MOT atoms to a magnetic trap. The atom cloud obtained in an UHV-MOT, is not suitable for directly loading to a magnetic trap. Magnetic trapping needs all the atoms to be in the trappable state having appropriate hyperfine quantum number and a suitably lower temperature of the cloud. Therefore, before transferring the atoms from UHV-MOT to a magnetic trap, preparation of the atom cloud in trappable state is necessary. To lower the temperature and increase the density of atoms in the UHV-MOT cloud, stages like compressed MOT and optical molasses are implemented. Subsequently, the optical pumping is implemented to accumulate most of the atoms in a suitable quantum hyperfine state (i. e. 5 $S_{1/2}|F=2, m_F=2\rangle$ of ^{87}Rb atom in our case).

To further lower the temperature of atom clouds obtained by laser cooling, evaporative cooling of atoms in the magnetic trap is a very promising method. In this method, the higher energy atoms from the trap are ejected by the application of radio frequency radiation, leading to a decrease in the temperature. Using the evaporative cooling process, the temperature can be lowered to reach the critical temperature to achieve the BEC of atoms (i.e. achieve phase-space density ~2.612).

5.1 Studies on phase-space density in the quadrupole magnetic trap

In this section, we discuss the studies on changes that occur in temperature, number density and phase-space density (ρ) when a laser cooled atom cloud from the molasses is instantaneously trapped in the quadrupole magnetic trap. The phase-space density (ρ) of atoms in the magnetic trap is of significant importance from the point of view of achieving BEC (which occurs at $\rho > 2.612$), whereas the number density governs the thermalization rate for the evaporative cooling. It was observed that the maximum value of ρ in the magnetic trap, after the atom cloud is transferred from molasses to the magnetic trap, depends upon the values of parameters such as temperature (T_i) and size of the atom cloud (σ_i) in the molasses and the magnetic field gradient of the magnetic trap. It has been shown that the temperature, number density and phase-space density of atom cloud in the quadrupole magnetic trap depend upon the value of magnetic field gradient *(b)* switched on instantaneously for trapping the laser cooled atom cloud in the quadrupole trap. The phase-space density in the magnetic trap ρ_f attains a maximum value at an optimum value of magnetic field gradient in the magnetic trap [28, 29].

The peak phase space density in the magnetic trap $\rho_f(0)$ is given as,

$$\rho_f(0) = \frac{N'(\mu_B b h)^3}{64\sqrt{2}\pi^{5/2} m^{3/2}} \frac{\left[\left(\frac{2mg}{\mu_B b}\right)^2 - 1\right]^2}{\left(\frac{k_B T_i}{3} + \kappa \mu_B b \sigma_i\right)^{9/2}}$$

where, N' is the number of atoms trapped in the quadrupole trap, m is the mass of atom, g is the acceleration due to gravity h is the Planck's constant and κ is the efficiency of transfer of atoms from molasses to quadrupole magnetic trap.

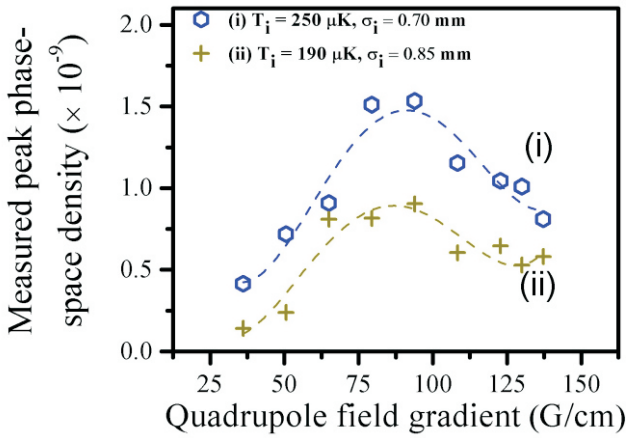

Fig. T.3.7: Measured variation in phase space density in the magnetic trap with the quadrupole field gradient for two sets of temperature and r.m.s. size of cloud after the molasses.

With increase in the b, $\rho_f(0)$ first increases and then decreases after attaining a maximum value at a certain field gradient b. The reduction in $\rho_f(0)$ after the maximum value is due to increase in the temperature of cloud in the magnetic trap and saturation in number density with b. The temperature attained finally in the magnetic trap increases with b due to increase in potential energy gained by the cloud from the trap. For lower values of b, the number density in the magnetic trap is low which results in lower values of $\rho_f(0)$. Therefore a maximum for $\rho_f(0)$ is obtained in its variation with the field gradient b. It was evident from these results that measured values of ρ in the magnetic trap also first increased with b and then decreased with it, after attaining a maximum value at an optimum b. We have demonstrated experimentally this behaviour for a set of temperature and size of the cloud (shown in Figure T.3.7). The results show that there is an optimum magnetic field gradient for which the achieved phase space density in the magnetic trap is maximum.

5.2 Formation of QUIC trap

The quadrupole trap though serves as the starting point for magnetic trapping, has a severe shortcoming of leakage from the centre of the trap. This shortcoming is removed by introducing another coil. After the initial switching-on of the quadrupole trap fields, the current in the quadrupole coils was slowly ramped to 23 A in 500 ms to form the quadrupole trap fully. After quadrupole coils current reaches the maximum value, current in Ioffe coil was slowly ramped from 0 to 19.5 A to convert quadrupole trap configuration into the QUIC trap configuration. The variation in the magnetic field of quadrupole coil, Ioffe coil, and the resultant field due to both coils with the position along the Ioffe coil axis are shown in Figure T.3.8.

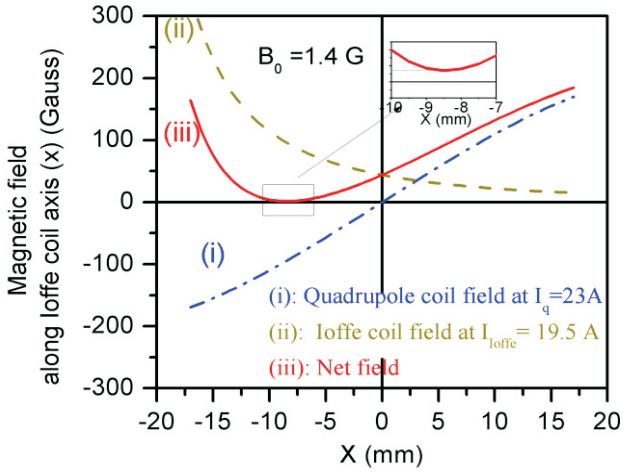

Fig. T.3.8: Variation in the magnetic field of quadrupole coil, Ioffe coil, and the resultant field due to both coils with the position along the Ioffe coil axis. The inset shows the non-zero field at the minima of the trap which removes the Majorana losses of atoms in trapped cloud.

5.3 Evaporative cooling and occurrence of BEC

For evaporative cooling of ^{87}Rb atoms trapped in our QUIC trap (shown in FigureT.3.9(a)), we apply radio frequency (RF) radiation emitted from a single loop antenna kept at one side of the glass cell with loop axis along the axis of quadrupole trap axis (z-axis).

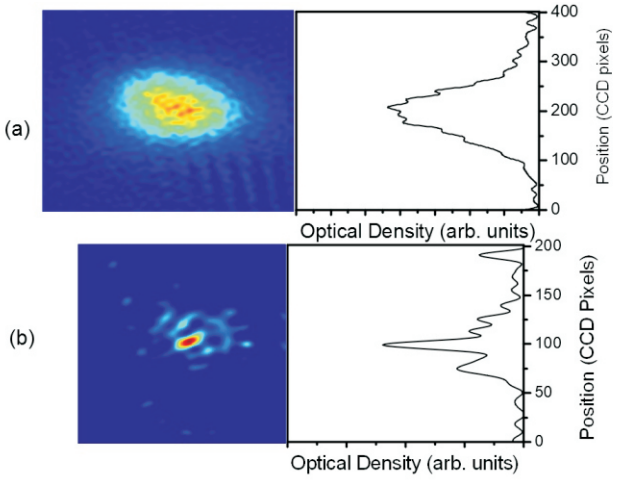

Fig. T.3.9: The optical density image and its density profile along the central line of the cloud for (a) cloud trapped in QUIC trap, (b) condensate after RF evaporation.

To scan the frequency of RF radiation, we used a logarithmic variation in frequency with time to achieve efficient evaporative cooling.

We have run a number of RF-evaporation cycles with different ranges of frequency scan and with different powers of RF source. After each run of RF-evaporation, the atom cloud was imaged by absorption probe imaging method and optical density image of the cloud was generated after processing of the absorption image of the cloud. The cloud was fitted with a bimodal distribution (composition of condensate and non-condensate part) to find out occurrence of BEC. The sharp peak at the centre of the cloud indicates occurrence of Bose condensate in the cloud as shown in Figure T.3.9.

6. Conclusion

The generation of ultracold samples of cold atoms serves a starting point for various atomic physics and atom optics applications. Here the description of a double-MOT setup comprising of VC-MOT and UHV-MOT is described. The setup was used to generate and manipulate samples of ^{87}Rb atoms having temperature in the regime of few hundred μK to few μK. The transfer of atoms between two MOTs using resonant and red-detuned push beam has been studied and presented. The UHV-MOT cloud was transferred to a magnetic trap formed by a quadrupole trap. The optimization of magnetic field gradient had been performed. Further, the atoms are trapped in the quadrupole-Ioffe configuration trap for removing the Majorana losses and achieving a longer life time suitable for evaporative cooling. The cloud trapped in the QUIC trap was subjected to RF evaporative cooling and Bose condensate formation was demonstrated in the cloud.

Acknowledgment

The work presented here is a part of Ph. D. thesis carried out under the supervision of Dr. S. R. Mishra, Head, LPAS. The author is thankful for his constant motivation and guidance. The author also thanks Shri S. K. Tiwari, Dr. S. Singh, Shri Vivek Singh and Dr. V. B. Tiwari, Head, Atom Optics Lab for their scientific and technical help. Thanks are also due to several members from Laser Controls & Instrumentation Division, Laser Components Design & Fabrication Section, RF systems Division and Ultra-high Vacuum Section for their support during the work. Author would like to thank Shri. H. S. Vora for providing the image processing software. Author would like to thank Dr. S. C. Mehendale, Dr. H. S. Rawat former heads of LPAS, Dr. P. D. Gupta, former Director for their support. Author would also like to thank Shri S. V. Nakhe, Director, LGB & MSGB and Dr. P. A. Naik, Director, RRCAT for their keen interest and support in the work.

References

[1] "*Advances in Atomic Physics: An Overview*", Claude Cohen-Tannoudji and David Guéry-Odelin, World Scientific, Hackensack, NJ, (2011).

[2] H. Perrin, P. Lemonde, F. P. dos Santos, V. Josse, B. L. Tolra, F. Chevy, and D. Comparat, *Comptes Rendus Physique* 12, 417 – 432 (2011).

[3] C. J. Bord´e, "Atomic interferometry and laser spectroscopy," in "Laser Spectroscopy X: Proceedings of the 10th International Conference," , M. Ducloy, E. Giacobino, and G. Camy, eds. (World Scientific Publishing Co Pte Ltd, Font-Romeu, France,, 1991).

[4] C. J. Bord´e, "Matter wave interferometers: a synthetic approach," in "*Atom Interferometry*", P. R. Berman, ed. (Academic Press Inc., CA, 1997), pp. 257–292.

[5] A. Peters, K. Y. Chung, and S. Chu, *Metrologia,* 38, 25–61 (2001).

[6] J. J. García-Ripoll, P. Zoller, and J. I. Cirac, *J. Phys. B: At. Mol. Opt. Phys.* 38, S567 (2005).

[7] "*Introduction to Quantum Optics*", G. Gilbert, A. Aspect, and C. Fabre, (Cambridge University Press, 2010).

[8] *J. Weiner, V. S. Bagnato, S. Zilio, and P. S. Julienne, Rev. Mod. Phys. 71, 1 (1999).*

[9] *"Cold Molecules: Theory, Experiment, Applications"*, R. Krems, B. Friedrich, and W. C. Stwalley, eds., (CRC Press, Taylor and Francis Group, 2009).

[10] *"Atom Optics"*, P. Meystre, (Springer, 2001).

[11] S. L. Rolston, *Physics*, 1, 2 (2008).

[12] *"Bose-Einstein Condensation in Atomic Gases"*, Proceedings of the International School of Physics "Enrico Fermi," Course CXL, Varenna, 1998, (edited by M. Inguscio, S. Stringari, and C. E. Wieman, IOS Press, Amsterdam, 1999).

[13] "*Bose-Einstein condensation in dilute gases*", C. J. Pethick and H. Smith, (Cambridge University Press, 2008), 2nd ed.

[14] *"Laser cooling and trapping"*, H. J. Metcalf and P. van der Straten, (Springer-Verlag New York, 1999).

[15] M. H. Anderson, J. R. Ensher, M. R. Matthews, C. E. Wieman, and E. A. Cornell, *Science* 269, 198–201 (1995).

[16] C. C. Bradley, C. A. Sackett, J. J. Tollett, and R. G. Hulet, *Phys. Rev. Lett*. 75, 1687 (1995). ibid. 79, 1170 (1997).

[17] K. B. Davis, M.-O. Mewes, M. R. Andrews, N. J. van Druten, D. S. Durfee, D. M. Kurn, and W. Ketterle, *Phys. Rev. Lett.* 75, 3969 (1995).

[18] W. Ketterle and N. J. van Druten, "Evaporative cooling of trapped atoms," *Adv. At. Mol. Opt. Phys.* 37, 181 (1996).

[19] C. J. Myatt, N. R. Newbury, R. W. Ghrist, S. Loutzenhiser, and C. E. Wieman, *Opt. Lett.* 21, 290 (1996).

[20] A. L. Migdall, J. V. Prodan, W. D. Phillips, T. H. Bergeman and H. J. Metcalf, *Phys. Rev. Lett*, 54, 2596, (1985).

[21] T. Esslinger, I. Bloch and T. W. Hänsch. *Phys. Rev. A* 58, R2664 (1998).

[22] S. R. Mishra, S. P. Ram, S. K. Tiwari and H. S. Rawat, *Pramana-J. Phys.* 88, 59 (2017).

[23] S. R. Mishra, S. P. Ram, S. K. Tiwari, and S. C. Mehendale, *Phys. Rev. A*, 77, 065402, (2008) and references therein.

[24] S. P. Ram, S. K. Tiwari, and S. R. Mishra, J. Korean Phys. Soc. 57, 1303 (2010) and references therein.

[25] S. P. Ram, S. R. Mishra, S. K. Tiwari, and S. C. Mehendale, *Rev. Sci. Instrum.*, 82, 126108, (2011).

[26] E. Dimova, O. Morizot, G. Stern, C. G. Alzar, A. Fioretti, V. Lorent, D. Comparat, H. Perrin, and P. Pillet, *Eur. Phys. J. D* 42, 299 (2007).

[27] S. P. Ram, S. K. Tiwari, S. R. Mishra, and H. S. Rawat , *Rev. Sci. Instrum.*, 84, 073102, (2013).

[28] S. P. Ram, S. K. Tiwari, S. R. Mishra and H. S. Rawat, *Pramana J. Phys.*, 82, 419, (2014).

[29] S. P. Ram, S. R. Mishra, S. K. Tiwari and H. S. Rawat, *J. Korean Phys. Soc.*, 65, 462, (2014).